

New Selective Phosphodiesterase 4D Inhibitors Differently Acting on Long, Short, and Supershort Isoforms

Olga Bruno,^{*,†} Alessia Romussi,[†] Andrea Spallarossa,[†] Chiara Brullo,[†] Silvia Schenone,[†] Francesco Bondavalli,[†] Nicolas Vanthuyne,[‡] and Christian Roussel[‡]

[†]Dipartimento di Scienze Farmaceutiche, University of Genoa, v.le Benedetto XV, 3-16132 Genoa, Italy, and [‡]UMR 6263, Laboratoire de Stéréochimie Dynamique et Chiralité Chirosciences, ISM2, University "Paul Cézanne", Marseille, France

Received February 25, 2009

The lack of selective inhibitors toward the long, short, or supershort phosphodiesterases (PDE4s) prevented researchers from carefully defining the connection between different enzyme isoforms, their brain localization, and their role in neurodegenerative diseases such as Alzheimer's disease (AD). In the search for new therapeutic agents for treating memory and learning disorders, we synthesized new rolipram related PDE4 inhibitors, which had some selectivity toward the long form PDE4D3. The first series was synthesized as racemate and then resolved by semipreparative HPLC on chiral supports. Herein we report the synthetic pathways to obtain compounds **1a–c**, **2a–c**, **3a–c**, **4a–f**, **5a,b**, **6a,b**, **7a,b**, the chiral analytical study to resolve compounds **1a–c**, **2a–c**, **3a–c**, the molecular docking study for compound **1c**, and the biological results and some SAR considerations that provide some insights and hints for the structural requirements for PDE4D subtype selectivity and enzyme inhibition.

Introduction

Cyclic adenosine monophosphate (cAMP^a) plays a pivotal role in several physiological events. In the central nervous system (CNS), cAMP controls the signal transduction cascade activated by neuron stimulation.¹ It is implicated in complex processes such as learning² and memory.³ Recently, the involvement of cAMP in the pathological events causing AD has been clearly demonstrated.^{4,5}

PDE4 specifically catalyze the hydrolysis of cAMP modulating the intracellular concentration of this second messenger. A number of biological and pharmacological studies have proven the involvement of PDE4 enzymes in memory processes and suggested that PDE4 inhibitors may be therapeutic agents for cognitive disorders. For example, PDE4 enzymes are involved in *N*-methyl-D-aspartate (NMDA) receptor-mediated signal transduction mechanisms. Rolipram is a known non-selective PDE4 inhibitor, able to reverse the amnesic effects of the NMDA antagonist MK-801 in rats and to enhance the NMDA-induced cAMP increase in rat's cortical neurons.^{6,7} Moreover, rolipram improves the learning ability of young rats^{8,9} and reverses scopolamine-induced cognitive deficits.^{10,11} The increase of cAMP levels, induced by a PDE4 inhibitor, enhances 5-hydroxytryptamine (5-HT) release and reverses

memory deficits induced by a lowered serotonin neurotransmission.¹² Rolipram antagonizes the memory impairment caused by a deficit in postsynaptic cAMP/protein kinase A/cAMP-response-element-binding (cAMP/PKA/CREB) pathway and counteracts the tendency of amyloid beta 42 peptide (A β 42) to suppress cAMP/PKA/CREB signaling cascade,¹³ as confirmed by an experimental murine model of AD.¹⁴ Recently, subchronic rolipram treatment was also reported to improve long-term memory performances in normal mice.¹⁵

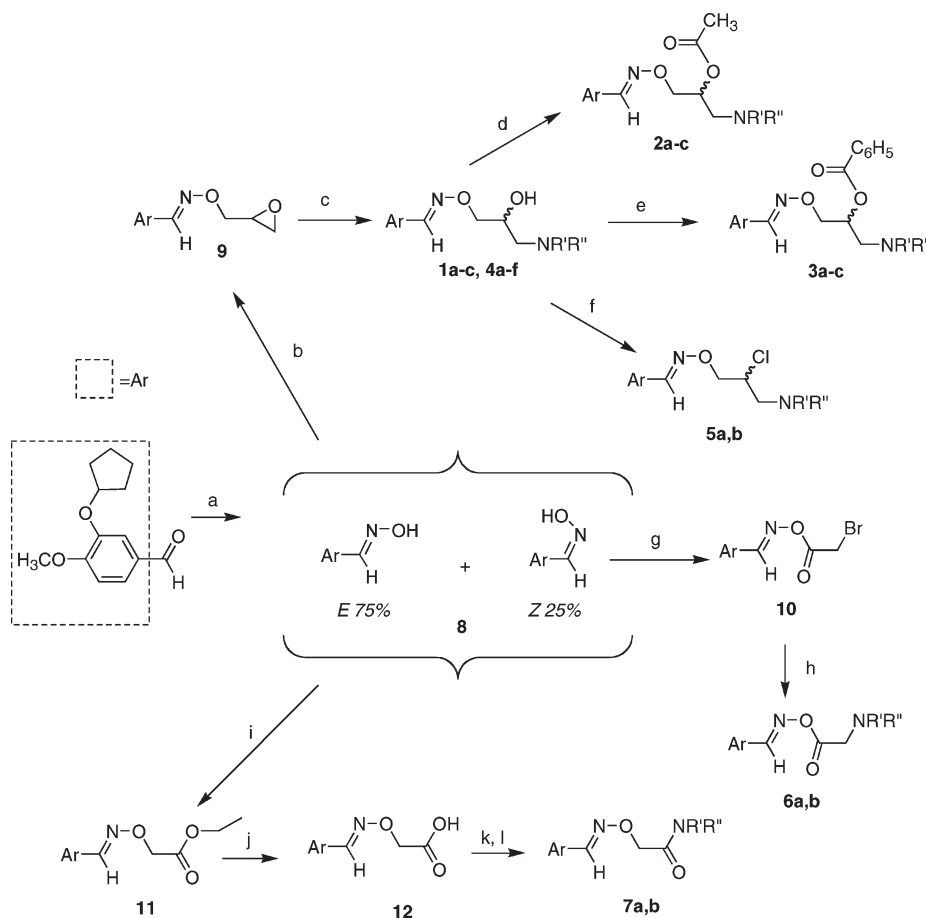
The four PDE4 genes encode for different enzyme isoforms (namely A, B, C, and D) further classified in 21 subtypes.^{16–18} On the basis of their primary structures, PDE4 can also be distinguished in "long", "short" or "supershort" enzymes.¹⁹ In particular, the long isoforms show two regulatory regions, upstream conserved region 1 and 2 (UCR1 and UCR2), inserted between the N-terminal portion and the catalytic domain. The protein kinase A (PKA) mediated phosphorylation of UCR1 domain activates PDE4 enzyme;²⁰ two phosphorylation sites for extracellular signal-regulated kinase (ERK) and phosphoinositide-3-kinase (PI3K) are also present in the catalytic domain (Ser579 and Ser239, respectively), further modulating enzyme activity.²¹ UCR1 domain is missing in the short forms, whereas the supershort forms not only lack UCR1 but also have a truncated UCR2 domain.

It is well-known that PDE4B and PDE4D (particularly PDE4D1–D5) are highly expressed in hippocampus and cortex regions, but it is to ascertain what isoforms are overexpressed in the different brain regions affected in AD patients.²²

The lack of selective inhibitors toward the long, short or supershort forms prevented a clear connection between the different isoforms, their brain localization, and biological function. The poor selectivity of rolipram toward the different PDE4 isoforms causes a series of central side effects

*To whom correspondence should be addressed. Phone: +39 010 353 8367. Fax: +39 010 353 8358. E-mail: obruno@unige.it.

^aAbbreviations: AD, Alzheimer disease; PDE2, PDE3, PDE4, PDE5, PDE6 phosphodiesterase type 2, 3, 4, 5, 6; cAMP, cyclic adenosine monophosphate; NMDA, *N*-methyl-D-aspartate; 5-HT, 5-hydroxytryptamine; cAMP/PKA/CREB, cAMP/protein kinase A/cAMP-response-element-binding; A β 42, amyloide beta 42 peptide; UCR1 and UCR2, upstream conserved region 1 and 2; PKA, protein kinase A; ERK, extracellular signal-regulated kinase; PI3K, phosphoinositide-3-kinase; α -TNF, alpha-tumor necrosis factor; HARBS, high affinity rolipram binding site.

Scheme 1. Synthesis of Compounds **1a–c**, **2a–c**, **3a–c**, **4a–f**, **5a,b**, **6a,b**, **7a,b**^a

^a Reagents: (a) NH₂OH·HCl, EtOH, rt, 4 h, then, H₂O, NaHCO₃; (b) Na, abs EtOH, rt, then epichlorohydrin, DMF, 45 °C, overnight; (c) HNR'R'', 45 °C, 12 h; (d) (CH₃CO)₂O, anhyd CH₃COONa, 45 °C, 3 h; (e) benzoyl chloride, Py, 45 °C, 5 h; (f) SOCl₂, anhyd TEA, rt, 5 h; (g) BrCH₂COBr, anhyd K₂CO₃, DCM, 0 °C; (h) HNR'R'', anhyd TEA, DCM, reflux, overnight; (i) BrCH₂COOEt, anhyd K₂CO₃, DCM, rt, then, reflux, overnight; (j) NaOH, EtOH/H₂O, 55 °C, 2 h; (k) SOCl₂, DCM, reflux, 4 h; (l) HNR'R'', DCM, 45 °C, 12 h.

(e.g., sedation, emesis), which complicate the understanding of its physiological action and prevent its use as a drug.

Recently, we reported a series of rolipram analogues as potential anti-inflammatory agents able to inhibit neutrophil activity.²³ These 3-cyclopentyloxy-4-methoxybenzaldehyde derivatives (e.g., compounds **1a–c**, see Scheme 1 and Table 1) inhibited the superoxide anion production in neutrophils stimulated with alpha-tumor necrosis factor (α-TNF), and this effect was related to a dose-dependent increase of cAMP levels. The most active compound (**1c**), screened on several enzymatic assays, resulted in PDE4 competitive antagonist with a high selectivity being inactive toward PDE3 and PDE5. The binding test on high affinity rolipram binding site (HARBS) showed a lower ratio PDE4-inhibition/rolipram binding affinity than rolipram (2.46 versus 152), evidencing a possible lack of side effects in vivo.

These encouraging results prompted us to select **1c** as lead compound for the development of a new series of PDE4 inhibitors which may be useful for treating neurodegenerative disorders.

In this new series of compounds, the 3-cyclopentyloxy-4-methoxyphenyl moiety was kept constant and modifications were applied to the linker chain and to the terminal amino group. Thus, in compounds **2**, **3**, and **5**, the hydroxy group of the propyl chain was either esterified (**2,3**) or replaced by a chlorine atom (**5**) to evaluate the effect of electronic and steric

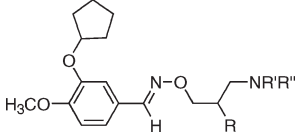
hindrance variation on the activity. The replacement of **1c** morpholine moiety with other basic portions led to derivatives **4**, while the shortening of the propyl chain led to compounds **6** and **7** (see Table 2).

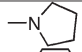
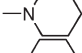
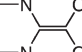
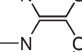
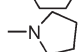
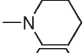
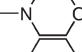
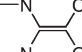
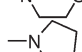
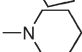
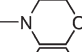
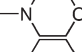
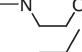
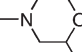
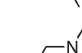

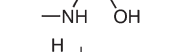
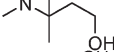
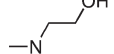
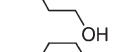
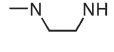
To assess the influence of the chiral center on the enzymatic interaction, we developed an analytical method of chiral HPLC and the racemic mixtures of **1c**, **2c**, and **3c** were resolved by semipreparative HPLC on chiral supports, as reported in the Experimental Section.

The racemates **1a–c**, **2a–c**, **3a–c**, **4a–f**, and the pure enantiomers **1c**(+), **1c**(–), **2c**(+), **2c**(–), **3c**(+), and **3c**(–) were tested on human PDE4 (see Table 1). Compounds **5a,b**, **6a,b**, and **7a,b** were tested on human PDE4D as racemic mixture (see Table 2).

The most active compounds **4a**, **5b**, **6b**, and **7b** were further tested on a panel of different PDE4 isoforms (namely A4, B2, C2, D1, D2, D3), considering them as the major representative (see Table 3). Compound **4a** was also tested on PDE1C, PDE2, PDE3, PDE5, and PDE6 to assess its selectivity profile.

To elucidate the bioactive conformation of compounds **1** inside the PDE4D binding site, a docking calculation was carried out on **1c**. The four possible **1c** isomers (namely, *E/R*, *E/S*, *Z/R* and *Z/S*) were considered independently. The docking complexes were calculated using the Autodock 3.05 program according to the procedure described in the Experimental Section.

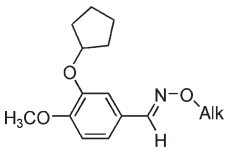
Table 1. Structure and PDE4 Inhibition of Compounds **1a–c**, **2a–c**, **3a–c**, **4a–f**, and Rolipram as Reference Compound^a


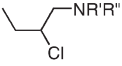
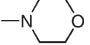
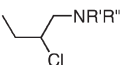
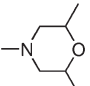
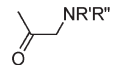

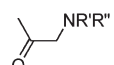
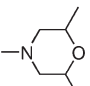
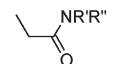
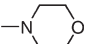
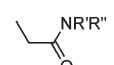
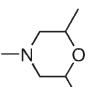
Comp.	R	NR'R''	PDE4 Inhibition% (10 μ M) ^a	IC ₅₀ (μ M)	95% Confidence intervals (μ M)
1a	OH		6	nd ^b	nd
1b	OH		20	nd	nd
1c	OH		81	3.23	2.04-5.11
1c(+)	OH		55	10.50	8.67-12.60
1c(-)	OH		69	4.49	3.40-5.92
2a	OCOCH ₃		31	nd	nd
2b	OCOCH ₃		28	nd	nd
2c	OCOCH ₃		68	3.98	2.35-6.70
2c(+)	OCOCH ₃		73	nd	nd
2c(-)	OCOCH ₃		70	nd	nd
3a	OCOPh		43	nd	nd
3b	OCOPh		40	nd	nd
3c	OCOPh		73	3.62	2.70-4.85
3c(+)	OCOPh		81	nd	nd
3c(-)	OCOPh		88	nd	nd
4a	OH		93	1.46	0.98-2.17
4b	OH		43	nd	nd
4c	OH		32	nd	nd
4d	OH		20	nd	nd
4e	OH		55	6.70	4.33-10.35
4f	OH		34	nd	nd
rolipram			-	0.41	na ^c

^a The PDE4 inhibition is expressed as % inhibition in respect to the control at 10 μ M, in duplicate, and as IC₅₀ (μ M) for active compounds. Fiducial intervals at 95% confidence are reported at μ M concentration. Cerep's protocol considers as inactive compounds having % inhibition inferior to 50%, thus the IC₅₀ values were not calculated for them. Active compounds were further tested at five concentrations in the interval 5×10^{-8} – 10^{-4} M, and the

Chemistry. Derivatives **4a–f** were prepared according to the procedures already reported for the synthesis of derivatives **1**.²³ Briefly, the reaction of hydroxylamine hydrochloride with 3-cyclopentyloxy-4-methoxybenzaldehyde, prepared by isovanillin's alkylation,²⁴ led to the 3-cyclopentyloxy-4-methoxybenzaldehyde oxime intermediate (**8**) as a

mixture of the two isomers (*E/Z*), one being preponderant (about 75%) (see Scheme 1). The two isomers were first separated by column chromatography (Silica gel, gradient of diethyl ether/petroleum ether 40–60 °C (1:1)) and characterized by elemental analysis and ¹H NMR spectral data (available on Supporting Information). In agreement with

Table 2. Structure and Recombinant Human PDE4D Inhibition of Compounds **5a,b**, **6a,b**, **7a,b**, and Rolipram as Reference Compound^a


Comp.	Alk	NR'R''	PDE4D % Inhibition (10 μ M)	IC ₅₀ (μ M)	95% Confidence intervals (μ M)
5a			72	5.91	2.34-15
5b			74	3.42	1.65-7.12
6a			42	nd ^b	nd
6b			32	nd	nd
7a			73	3.48	1.00-12.1
7b			84	0.67	0.225-2.02
Rolipram			na ^c	0.092	na

^a The PDE4D inhibition is expressed as % inhibition in respect to the control at 10 μ M, in duplicate, and as IC₅₀ (μ M) for active compounds. Fiducial intervals at 95% confidence are reported at μ M concentration. Only compounds showing control inhibition higher than 50% were further tested at five

Table 3. Inhibition Activity toward Different PDE4 Isoforms of Compound **4a**, **5b**, **6b**, **7b**, and Rolipram as Reference Compound^a

PDE4 isoforms	compounds				
	4a	5b	6b	7b	rolipram
PDE4A4	34	37	5	34	79
PDE4B2	39	24	14	23	65
PDE4C2	19	35	10	25	57
PDE4D1	54	41	11	57	78
PDE4D2	53	62	15	76	80
PDE4D3	68	69	20	67	79

^a The results are expressed as % inhibition in respect to the control at 10 μ M concentration, in duplicate.

literature data,²⁵ we assigned the *E* configuration to the predominant compound which showed the aldehyde proton signal at 8.01 ppm, shifted 0.41 units to high fields with respect to the other isomer, owing to the paramagnetic shift induced by hydroxy group on the aldehyde proton. Because all the attempts to separate **8** *E* and *Z* isomers by HPLC failed, we carried out a quantitative photodensitometric analysis, after TLC separation, that evidenced the presence of 75% of *E* and 25% of *Z* isomer, as reported in the Experimental Section.

Then the oxime (**8**) was reacted as a *E/Z* mixture with epichlorohydrin to give the intermediate epoxide (**9**) that was reacted, without purification, with the suitable amines to give compounds **1a–c** and **4a–f** (see Scheme 1). All the

compounds were obtained as theoretical mixture of four diastereoisomers (*E/R*, *E/S*, derived from *E* oxime; *Z/R* and *Z/S* derived from *Z* oxime) in percentages not detectable by nonchiral analytical methods. Compounds **2a–c** and **3a–c** were prepared by acylation of the corresponding alcohols **1**, with acetic anhydride or benzoyl chloride, respectively (see Scheme 1). The chiral HPLC separation of compounds **1c**, **2c**, and **3c** evidenced the prevalence of the more stable *E* isomers with a very small amount of *Z* isomers (see Experimental Section). After storage in different conditions (solvent, temperature), the mixtures were again analyzed by chiral HPLC and no increase of *Z* isomers was remarked (data not reported).

Compounds **5a,b** were obtained from the corresponding alcohols **1c** and **4a**, respectively, with thionyl chloride in dichloromethane (see Scheme 1).

The reaction of **8** with bromoacetyl bromide, in the presence of anhydrous K₂CO₃, at 0 °C, led to intermediate **10** that was treated with morpholine or 2,6-dimethylmorpholine to yield compounds **6a,b** (see Scheme 1).

Finally, compounds **7a,b** were prepared starting from **8** that reacted with 2-bromoacetic acid ethyl ester to give the intermediate (**11**) that was then hydrolyzed in NaOH/ethanol medium; the so obtained carboxylic acid (**12**) was activated in the corresponding acyl chloride and reacted with the proper amines to yield the desired compounds **7a**, **b** (see Scheme 1).

Table 4. IC₅₀ (μM) Values of Compounds **4a**, **5b**, **7b**, and Rolipram, as Reference Compound, Determined in Duplicate toward PDE4D3^a

compd	IC ₅₀ (μM)	95% confidence intervals (μM)
4a	3.46	2.18–7.32
5b	4.27	2.02–8.34
7b	1.91	0.65–7.01
rolipram	0.4–1.8	na ^b

^a Fiducial intervals at 95% confidence are reported at μM concentration. Compounds were tested at five concentrations in the interval 5×10^{-8} – 10^{-4} M, and the IC₅₀ values were determined by nonlinear regression analysis of inhibition curve using Hill equation curve fitting (Graph Pad Prism, San Diego, CA). ^b na = not available

Table 5. IC₅₀ (μM) and K_i (μM) Values^a for Compound **4a** and Rolipram, as Reference Compound, against PDE4D1, PDE4D2, and PDE4D3

enzyme	substrate (cAMP) conc (μM)	substrate (cAMP) K _m (μM)	4a	rolipram	4a	rolipram
			IC ₅₀ (μM)	IC ₅₀ (μM)	K _i (μM)	K _i (μM)
PDE4D1	1	1.2	7.09	0.91	3.86	0.49
PDE4D2	1	4	9.18	1.17	7.34	0.93
PDE4D3	1	1.2	2.86	0.55	1.55	0.30

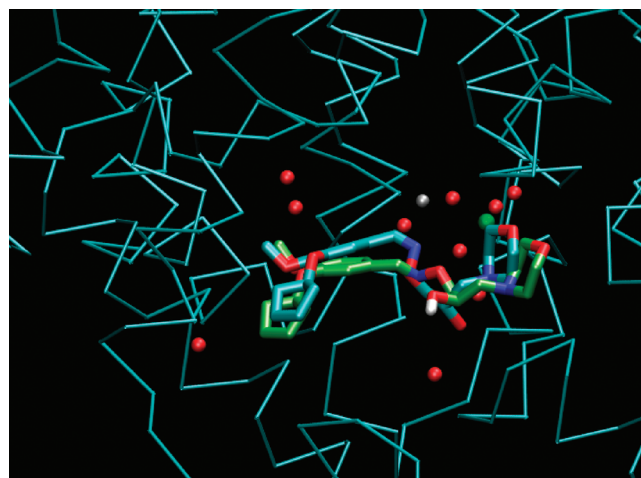
^a Compound **4a** and rolipram, as reference compound, were tested at six concentrations in the interval 5×10^{-9} – 10^{-4} M, and the IC₅₀ values were determined by nonlinear regression analysis of inhibition curve (Graph Pad Prism, San Diego, CA). The K_i values were derived from the IC₅₀ values using the Cheng–Prusoff equation: $IC_{50} = K_i (1 + [S]/K_m)$.

Enzymatic Assays. All the synthesized compounds (**1a–c**, **2a–c**, **3a–c**, **4a–f**, **5a,b**, **6a,b**, **7a,b**) were tested on human PDE4 (Table 1) or PDE4D enzymes (Table 2) by CEREP (Celle L'Evescault, France) following standard procedures,^{26,27} as briefly described in Experimental Section. The compounds were initially screened at 10 μM concentration, then only those derivatives showing more than 50% control inhibition were tested at further concentrations to determine the IC₅₀ values. Compounds **1c**, **2c**, and **3c** were tested both as racemic mixtures and as pure *E*(+) and *E*(–) enantiomers (Table 1).

Compounds **4a**, **5b**, **6b**, and **7b**, which showed the best IC₅₀ values in the preliminary PDE4 or PDE4D tests, were then submitted to a large screening on a panel of different PDE4 isoforms (A4, B2, C2, D1, D2, D3) to assess its ability to discriminate between them (see Tables 3 and 4). Compound **4a** was further tested on other phosphodiesterase types (PDE1C, PDE2, PDE3, PDE5, and PDE6) to verify its selectivity (data not reported). The selectivity studies were performed by Scottish Biomedical (Glasgow, UK) following the procedures described in Experimental Section.

Results. Among the first synthesized compounds (**1**, **2**, **3**), the morpholine derivatives **1c**, **2c**, and **3c** were PDE4 inhibitors at μM concentration, while the pyrrolidinyl and piperidinyl analogues were completely inactive. The corresponding pure enantiomers **1c**(*E*,+), **1c**(*E*,–), **2c**(*E*,+), **2c**(*E*,–), **3c**(*E*,+), and **3c**(*E*,–) also showed a good PDE4 inhibition at 10 μM concentration; however, while no significant change in activity was observed between (+) and (–) enantiomers of the acetyl (**2c**) and benzoyl (**3c**) derivatives and their racemic forms, **1c**(+) was slightly less active than **1c**(–) and they both were less active than their racemic form (Table 1).

In the second series (compounds **4a–f**), only the 2,6-dimethylmorpholine derivative **4a** and the diethanolamine derivative **4e** were active toward PDE4 enzyme. Particularly, compound **4a** showed an increase, whereas **4e** had a decrease

**Figure 1.** Docking models of enantiomers **1c**(*E*/*R*) (pale-green sticks) and **1c**(*Z*/*S*) (light-blue sticks) inside the PDE4D active site. The protein is displayed as Cα trace. Water molecules are shown as red spheres, Zn²⁺ and Mg²⁺ metal ions are shown as gray and green spheres, respectively.

of activity in comparison with the previous compounds. All the others having different amine residues (3-morpholin-4-yl-propylamino, 1-methyl-ethanolamino, 2,2'-dimethyl-ethanolamino, piperazinyl) were inactive (Table 1).

5a,b, having a chlorine atom instead of a hydroxy group in the propyl chain, were less active than the corresponding alcohols **1c** and **4a** both on the PDE4D test and on the more specific PDE4D3 test (Tables 2 and 4).

6a,b, bearing the carbonyl group adjacent to the oxime oxygen, were slightly active at 10 μM concentration toward PDE4D, but this activity was not further confirmed in the following tests. **7a,b** with the carbonyl function near to the amine nitrogen, showed a good activity toward PDE4D, **7b** being the most active among the whole series of compounds.

In the preliminary screening on different PDEs and PDE4 isoforms, **4a** evidenced a good selectivity (Table 3): it inhibited the longform PDE4D3 at good level, the short and supershort PDE4D1 and PDE4D2 with potency around 50%; it was inactive toward the other isoforms PDE4A4, PDE4B2, PDE4C2, and the other PDEs (PDE1C, PDE2, PDE3, PDE5, PDE6, data not shown).

The other compounds **5b**, **6b**, and **7b** showed a different behavior. **5b** and **7b** inhibited at good level PDE4D3 and PDE4D2, while the action on PDE4D1 was not relevant (41% and 57% of inhibition, respectively); they were inactive on PDE4A4, PDE4B2, and PDE4C2 enzymes; **6b** was completely inactive toward all the tested isoforms (Table 3). The IC₅₀ determination against PDE4D3 confirmed **5b** and **7b** as less and more active than **4a**, respectively (Table 4).

The radiometric study performed on PDE4D3, PDE4D2, and PDE4D1 showed that **4a** is PDE4D antagonist, with greater potency toward PDE4D3 in respect to PDE4D1 and PDE4D2 (see IC₅₀ and K_i values on Table 5) being the ratio PDE4D1 K_i/PDE4D3 K_i = 2.5 and PDE4D2 K_i/PDE4D3 K_i = 4.7. It is worth mentioning that the same values calculated for rolipram were 1.6 and 3.1, respectively, confirming the higher selectivity of **4a**.

Docking Study, SAR, and Discussion. According to the docking results, out of the four isomers considered, only isomers *E*/*R* and *Z*/*S* were predicted to assume a bioactive

conformation in keeping with the crystallographic data collected for other PDE4 inhibitors embedding the 3-cyclopentyl-oxy-4-methoxyphenyl moiety.

The PDE4D/**1c**(*E/R*) complex is stabilized by a number of hydrophobic contacts involving the 3-cyclopentyl-oxy-4-methoxyphenyl moiety and Tyr159, Asn321, Ile336, Phe340, and Gln369 side chains. The linker is marginally involved in complex stabilization, whereas the morpholine ring establishes van der Waals contacts with Asn209, Asp272, and Met273. Furthermore, the morpholine oxygen atom is hydrogen bonded to Asn209 side chain amide nitrogen (distance 2.9 Å) and to the carboxylic group of Asp272 (distance 2.7 Å).

Differently from the above-described model, in the PDE4D/**1c**(*Z/S*) complex, the ligand linker is deeply involved in complex stabilization. The hydroxy group would be hydrogen bonded to two water molecules (namely 1202 and 1105) directly connected to the metal ions in the active site. Furthermore, the hydroxy group is in contact with Ser208 side chain. The morpholine ring interacts with Glu230 and Asn209 side chains, moreover the morpholine oxygen would be hydrogen bonded to Met273 main chain NH group and to Asp272 carboxylic functionality. Further stabilization to this complex is provided by hydrophobic contacts involving the 3-cyclopentyl-oxy-4-methoxyphenyl moiety and Met357, Phe340, Gln369, Phe372, Tyr159, Asn321, and Phe372. A feature of these interactions was reported in Figure 1.

This docking study predicted a good interaction with a catalytic domain of PDE4D for **1c**(*E,R*) and **1c**(*Z,S*) isomers. Because the *Z* isomers were not recovered and the absolute configuration of **1c**(*E,+*) and **1c**(*E,-*) was not defined, at the moment it is difficult to confirm the docking prediction on the basis of enzymatic activity. Moreover, the lack of crystallographic data on the regulatory UCR1 domain, which is present only in the PDE4 longforms, limits the understanding of the activity and selectivity profile of our compounds that can be rationalized only by the SAR considerations.

On the basis of enzymatic results, we can underline some structural features responsible for PDE4 inhibitory activity as well as PDE4D3 selectivity. The morpholinyl substructure at the end of the propyl chain is fundamental for the inhibitory activity. In fact, other tertiary (pyrrolidine, piperidine, piperazine) or secondary (i.e., methyl-ethanolamine, 2,2'-dimethyl-ethanolamine) amino groups gave inactive compounds, while the diethanolamine (mimicking an open morpholine ring) **4e** was active, although less than all the morpholine derivatives. The introduction of two methyl groups in the morpholine always increases the activity (see compounds **4a**, **5b**, **7b**).

The propyl-chain branching is essential for activity (compounds previously synthesized with linear chain were inactive),²³ but the role of the different substituents in the chiral center is very difficult to rationalize. Compounds with a free hydroxy group (**1c**, **4a**) were highly active but also the acetyl or benzoyl esters (**2c**, **3c**) showed a good inhibitory activity, thus the presence of a hydrogen atom responsible for hydrogen bond is not absolutely necessary.

The pure enantiomers of **2c** and **3c** showed enzymatic inhibition quite similar to the corresponding racemate, while the pure alcohol **1c**(*E,-*) is more active than the pure **1c**(*E,+*), but the differences observed in respect to the racemate are not enough to confirm the presence of an eutomer form.

The introduction of an electron-withdrawing substituent in the propyl chain fairly decreases the activity on PDE4D and also in PDE4D3.

The chain lengthening is detrimental for the activity (3-morpholin-4-yl-propylamino derivative **4b** was inactive), whereas the replacement of the branched propyl chain with the shorter oxoethyl chain (derivatives **6** and **7**) differently affects activity, according to the position of the carbonyl group. In fact, compounds **6a,b** were completely inactive toward all the PDE4 tested, whereas compounds **7a,b** inhibited PDE4D at good level.

Conclusions. We reported the synthesis and the biological and analytical studies of new 3-cyclopentyl-oxy-4-methoxybenzaldehyde derivatives which were good PDE4 inhibitors, compounds **7b** and **4a** being the most active ones. All the compounds, except **6a,b**, were selective PDE4D inhibitors, being almost inactive toward PDE4A4, PDE4B2, and PDE4C2 enzymes. Compound **4a** showed the most interesting profile, having a good PDE4 inhibition ($IC_{50} = 1.46 \mu M$, see Table 1) and a good selectivity toward the longforms PDE4D3. Anyway, it is noteworthy the very different behavior of compound **4a** in respect to rolipram, which inhibited quite indifferently all the PDE4 isoforms (Table 3). As far as we know, no other PDE4D inhibitors with the same biological profile have been reported in the literature until now.

In addition, we remark that even little structural modifications strongly affect the selectivity toward the different PDE4D isoforms. The SAR informations herein reported provide some suggestions to have PDE4 inhibitors able to distinguish among different PDE4D isoforms. Because they are the most expressed in hippocampal region, that is the brain area mainly involved in cognitive and memory diseases, these compounds would represent useful pharmacological tools to increase the knowledge on the role of PDE4D in neurodegenerative pathologies.

Experimental Section. Chemistry. Chemical Materials and Methods. All chemicals were purchased from Sigma-Aldrich srl (Milan, Italy). All the amines were purified by distillation before the use.

Melting points are not "corrected" and were measured with a Büchi 540 instrument. IR spectra were recorded with a Perkin-Elmer 398 spectrophotometer. ¹H NMR spectra were recorded on a Varian Gemini 200 (200 MHz) instrument; chemical shifts are reported as δ (ppm) relative to tetramethylsilane (TMS) as internal standard; signals were characterized as s (singlet), d (doublet), t (triplet), m (multiplet), br s (broad signal); *J* in Hz.

All compounds were tested for purity by TLC (Kieselgel 60F254 DC-Alufolien, E. Merck, Darmstadt, Germany).

Elemental analyses were determined with an elemental analyzer EA 1110 (Fison-Instruments, Milan, Italy) and the purity of all synthesized compounds was >95%.

General Procedure for 3-(Cyclopentyl-oxy)-4-methoxybenzaldehyde O-(2-Hydroxy-3-amin/cycloamin-1-ylpropyl)oximes (1a-c**, **4a-f**).** The procedure already reported for compounds **1a-c**²³ has been modified as follows to increase the reaction yields. To intermediate crude epoxide **9** (1.45 g, 5 mmol), an excess of the suitable amine (5 mL) was added and the reaction mixture was stirred for 18 h at 40–50 °C, monitoring the formation of the product by TLC. After cooling, the mixture was diluted with diethyl ether (10 mL), washed twice with water, and extracted three times with 1N HCl solution. The combined aqueous phases were made alkaline with 1 M NaOH solution and extracted three times

with CHCl_3 . The organic layer was dried (MgSO_4), filtered, and evaporated to give yellowish oils. Amines in excess were distilled under vacuum. The obtained crude oils were purified as follows: compound **4a** was chromatographed on silica gel (hexane/diethyl ether (5:95)) and then precipitated as hydrochloride; compounds **4b**, **4c**, **4d** were crystallized from diethyl ether; compound **4e** was precipitated as hydrochloride.

In the case of piperazine derivative (compound **4f**), the procedure was modified as follows: to a solution of piperazine (2.06 g, 3.98 mmol) in absolute ethanol (6 mL), warmed at 45–50 °C, the epoxide **9** (1.16 g, 3.98 mmol) in absolute ethanol (2 mL) was added dropwise. The reaction mixture was stirred at 45–50 °C for 2 h. After cooling, the mixture was treated as above-mentioned to give an oil that was purified by chromatography on silica gel (methanol/chloroform (5:90)). Compound **4f** was characterized as dihydrochloride.

Analytical Data of 3-(Cyclopentylloxy)-4-methoxybenzaldehyde O-[3-(2,6-Dimethyl-morpholin-4-yl)-2-hydroxypropyl]-oxime (4a). Yield 79%; mp for $\text{C}_{22}\text{H}_{34}\text{N}_2\text{O}_5 \cdot \text{HCl}$ 110 °C. ^1H NMR (CDCl_3): δ 1.05 (d, $J = 6.0$ Hz, 3H, CH_3 morph), 1.09 (d, $J = 6.2$ Hz, 3H, CH_3 morph), 1.49–2.02 (m, 10H, 4 CH_2 cyclopent + N- CH_2), 2.29–2.44 and 2.50–2.82 (2m, 4H, 2 N- CH_2), 3.50–3.70 (m, 2H, 2 CH morph), 3.79 (s, 3H, OCH_3), 3.91–4.24 (m, 3H, CH_2 + CH-OH), 4.67–4.80 (m, 1H, CH cyclopent), 6.78–7.15 (3m, 3H, Ar), 7.97 (s, 1H, CH=N). IR (KBr): cm^{-1} 3400–3200 (OH). Anal. Calcd for $\text{C}_{22}\text{H}_{34}\text{N}_2\text{O}_5 \cdot \text{HCl}$.

General Procedure for 2-([3-(Cyclopentylloxy)-4-methoxyphenyl]methylene)amino)oxy]-1-(cycloamin-ylmethyl) Ethyl Acetates (2a–c). To a solution of the suitable amino-alcohols (**1a–c**) (1.93 mmol) in acetic anhydride (2 mL) anhydrous sodium acetate (0.2 g, 2.44 mmol) was added and the mixture was stirred for 3–5 h at 40–50 °C, monitoring the formation of the product by TLC. After cooling, the mixture was poured into water and extracted three times with CHCl_3 . The combined organic layers were washed twice with 1 M NaOH solution and then several times with water, dried (MgSO_4), filtered, and evaporated to give yellow oils which were chromatographed on Florisil (100–200 mesh) (diethyl ether).

Analytical Data of 2-([3-(Cyclopentylloxy)-4-methoxyphenyl]methylene)amino)oxy]-1-(morpholin-4-ylmethyl) Ethyl Acetate (2c). Yield 81%. ^1H NMR (CDCl_3): δ 1.40–1.95 (m, 8H, 4 CH_2 cyclopent), 1.99 (s, 3H, CH_3), 2.30–2.60 (m, 6H, 3 N- CH_2), 3.60 (t, $J = 4.6$, 4H, 2 O- CH_2 morph), 3.78 (s, 3H, OCH_3), 4.10–4.32 (m, 2H, O- CH_2), 4.70–4.80 (m, 1H, CH cyclopent), 5.18–5.31 (m, 1H, CHOCOCH_3), 6.74 (d, $J = 8.0$ Hz, 1H, H-5 Ar), 6.95 (dd, $J = 1.8, 8.4$ Hz, 1H, H-6 Ar), 7.14 (d, $J = 1.8$ Hz, H-2 Ar), 7.92 (s, 1H, CH=N). IR (film): cm^{-1} 1738 (C=O). Anal. Calcd for $\text{C}_{22}\text{H}_{32}\text{N}_2\text{O}_6$.

General Procedure for 2-([3-(Cyclopentylloxy)-4-methoxyphenyl]methylene)amino)oxy]-1-(cycloamin-ylmethyl) Ethyl Benzoates (3a–c). To a solution of the suitable amino-alcohols (**1a–c**) (1.6 mmol) in pyridine (2 mL) benzoylchloride (0.3 mL, 2.24 mmol) was added and the reaction solution was stirred for 16 h at 40–50 °C. After cooling, the reaction mixture was diluted with CHCl_3 (10 mL), washed three times with 1N HCl solution, and then several times with water. The organic layer was dried (MgSO_4), filtered, and evaporated to yield yellow oils which were chromatographed on Florisil (100–200 mesh) (diethyl ether).

Analytical Ddata of 2-([3-(Cyclopentylloxy)-4-methoxyphenyl]methylene)amino)oxy]-1-(morpholin-4-ylmethyl) Ethyl Benzoate (3c). Yield 70%. ^1H NMR (CDCl_3): δ 1.30–1.95 (m, 8H, 4 CH_2 cyclopent), 2.30–2.78 (m, 6H, 3 CH_2 -N), 3.60 (t, $J = 4.6$ Hz, 4H, 2 O- CH_2 morph), 3.78 (s, 3H, OCH_3), 4.25–4.50 (m, 2H, O- CH_2), 4.57–4.75 (m, 1H, CH cyclopent), 5.39–5.56 (m, 1H, CHOCOPh), 6.70 (d, $J = 7.8$ Hz, 1H, H-5 Ar), 6.91 (dd, $J = 1.6, 7.8$ Hz, 1H, H-6 Ar), 7.12 (d, $J = 1.6$ Hz, H-2 Ar), 7.20–7.57 and 7.89–8.10 (2m, 6H, 5 H benzoyl + CH=N). IR (film): cm^{-1} 1714 (C=O). Anal. Calcd for $\text{C}_{27}\text{H}_{34}\text{N}_2\text{O}_6$.

General Procedure for 3-(Cyclopentylloxy)-4-methoxybenzaldehyde O-[2-Chloro-3-(cycloamin-4-yl)propyl]-oxime (5a, b). To a solution of the appropriate amino-alcohol (**1c**, **4a**) (3.12 mmol) in dichloromethane (3 mL) anhydrous triethylamine (0.43 mL, 3.12 mmol) and thionyl chloride (0.27 mL, 3.74 mmol) were added dropwise at room temperature. After the addition the mixture was stirred at rt for 4 h. The solvent and excess thionyl chloride were removed under vacuum, the residue was diluted with dichloromethane (10 mL) and washed three times with water; the organic layer was dried (MgSO_4), filtered, and evaporated to give an oil which was purified by chromatography on silica gel (chloroform/hexane (9:1)).

Analytical Data of 3-(Cyclopentylloxy)-4-methoxybenzaldehyde O-[2-Chloro-3-(morpholin-4-yl)propyl]-oxime (5a). Yield 70%. ^1H NMR (CDCl_3): δ 1.50–2.05 (m, 8H, 4 CH_2 cyclopent), 2.60–2.91 (m, 4H, 2 CH_2 morph), 2.95–3.13 (m, 1H, CH), 3.48–3.79 (m, 6H, 2 CH_2 morph + CH_2), 3.84 (s, 3H, OCH_3), 4.22–4.45 (m, 2H, CH_2 -O), 4.70–4.85 (m, 1H, CH cyclopent), 6.80 (d, $J = 8.4$ Hz, 1H, H-5 Ar), 6.98 (dd, $J = 2.2, 8.4$ Hz, 1H, H-6 Ar), 7.18 (d, $J = 2.2$ Hz, H-2 Ar), 7.98 (s, 1H, CH=N). Anal. Calcd for $\text{C}_{20}\text{H}_{29}\text{ClN}_2\text{O}_4$.

Synthesis and Analytical Data of 3-(Cyclopentylloxy)-4-methoxybenzaldehyde O-(2-Bromoacetyl)oxime (10). To a mixture of 3-(cyclopentylloxy)-4-methoxybenzaldehyde oxime **8** (1.45 g, 6.16 mmol) solved in dichloromethane (6 mL) and anhydrous potassium carbonate (1.70 g, 12.32 mmol) cooled at 0–5 °C, a solution of bromoacetyl bromide (0.64 mL, 7.39 mmol) in dichloromethane (2 mL) was added dropwise, over 20 min period, with stirring. After the addition, the mixture was filtered and the residue washed several times with dichloromethane; the filtrate was evaporated under vacuum to yield a yellowish solid that was washed more times with diethyl ether, giving a white solid.

Yield: 84%; mp 126 °C. ^1H NMR (CDCl_3): δ 1.40–2.12 (m, 8H, 4 CH_2 cyclopent), 3.87 (s, 3H, OCH_3), 3.97 (s, 2H, CH_2Br), 4.71–4.90 (m, 1H, CH cyclopent), 6.86 (d, $J = 8.2$ Hz, 1H, H-5 Ar), 7.15 (dd, $J = 2.0, 8.2$ Hz, 1H, H-6 Ar), 7.32 (d, $J = 2.0$ Hz, 1H, H-2 Ar), 8.28 (s, 1H, CH=N). IR (KBr): cm^{-1} 1768 (C=O). Anal. Calcd for $\text{C}_{15}\text{H}_{18}\text{BrNO}_4$.

General Procedure for 3-(Cyclopentylloxy)-4-methoxybenzaldehyde O-(2-Cycloamino-acetyl)oximes (6a,b). To a suspension of suitable amine (morpholine or 2,6-dimethylmorpholine) (5.05 mmol, 1.5 equiv), anhydrous potassium carbonate (0.86 g, 6.7 mmol, 2 equiv) and potassium iodide (0.02 g, 0.10 mmol, 0.03 equiv) in dichloromethane (4 mL), the intermediate **10** (1.2 g, 3.37 mmol, 1equiv), solved in dichloromethane (2 mL), was added dropwise. The reaction mixture was refluxed for 3 h. After cooling, the mixture was filtered and the residue was washed several times with dichloromethane; the solvent was evaporated under reduced pressure and the obtained oil was diluted with diethyl ether, washed with water, and extracted

Table 6. Data for the Chiral HPLC Separations of the Different Racemates at 25 °C, 1 mL/min, UV 254 nm, and Polarimeter

compd	column type (250 mm × 4.6 mm)	mobile phase	R_{t1} (min)	R_{t2} (min)	k_1	k_2	α
1a	Chiralcel OD-H	hexane/isopropyl alcohol 8:2	29.13	55.48	8.71	17.49	2.01
	Chiralpak AS	hexane/isopropyl alcohol 8:2	8.95		1.98		
	Chiralpak AD	hexane/isopropyl alcohol 8:2	6.64		1.21		
	Chiralcel OB-H	hexane/ethanol 1:1	3.90		0.3		
	Chiralcel OJ	hexane/ethanol 1:1	4.19		0.39		
1b	Chiralcel OD-H	hexane/isopropyl alcohol 8:2	18.45	36.09	5.15	11.03	2.14
	Chiralpak AS	hexane/isopropyl alcohol 8:2	8.02		1.67		
	Chiralpak AD	hexane/isopropyl alcohol 8:2	6.33		1.11		
	Chiralcel OB-H	hexane/ethanol 1:1	3.82		0.27		
	Chiralcel OJ	hexane/ethanol 1:1	4.17		0.39		
1c	Chiralcel OD-H	hexane/isopropyl alcohol 8:2	23.67 (+)	43.63 (−)	6.89	13.54	1.97
	Chiralcel OD-H	hexane/isopropyl alcohol 3:7	8.37 (+)	13.19 (−)	1.79	3.40	1.90
	Chiralpak AS	hexane/isopropyl alcohol 8:2	10.72	11.97	2.57	2.99	1.16
	Whelk-01 (S,S)	hexane/isopropyl alcohol 1:1	17.53		4.84		
	Chiralpak AD	hexane/isopropyl alcohol 8:2	9.40		2.13		
2a	Chiralcel OD-H	hexane/isopropyl alcohol 8:2	6.41	21.15	1.14	6.05	5.32
2b	Chiralcel OD-H	hexane/isopropyl alcohol 8:2	5.86	11.01	0.95	2.67	2.81
2c	Chiralcel OD-H	hexane/isopropyl alcohol 8:2	13.06 (+)	64.41 (−)	3.35	20.47	6.11
	Chiralcel OD-H	Ethanol	5.81 (+)	14.58 (−)	0.93	3.86	4.15
3a	Chiralcel OD-H	hexane/isopropyl alcohol 8:2	6.81 (−)	19.80 (+)	1.27	5.60	4.41
3b	Chiralcel OD-H	hexane/isopropyl alcohol 8:2	6.70 (−)	10.93 (+)	1.23	2.64	2.14
3c	Chiralcel OD-H	hexane/isopropyl alcohol 8:2	14.63 (−)	92.51 (+)	3.88	29.84	7.69
	Chiralcel OD-H	ethanol	6.37 (−)	21.23 (+)	1.12	6.07	5.41

Table 7. Data for the Best Separation Conditions for **1c**, **2c**, **3c**^a

compd	column type (250 mm × 4.6 mm)	mobile phase	R_{t1} (min)	R_{t2} (min)	k_1	k_2	α
1c	Chiralcel OD-H	hexane/isopropyl alcohol (3/7)	8.37 (+)	13.19 (−)	1.79	3.40	1.90
2c	Chiralcel OD-H	ethanol	5.81 (+)	14.58 (−)	0.93	3.86	4.15
3c	Chiralcel OD-H	ethanol	6.37 (−)	21.23 (+)	1.12	6.07	5.41

^a Data are for analytical conditions that were scaled up for semipreparative separations.

three times with 1N HCl. The aqueous phase was made alkaline with NaHCO₃ saturated solution and extracted three times with chloroform; the organic extracts were washed three times with water, dried (MgSO₄), filtered, and evaporated under reduced pressure to yield yellowish oils that crystallize by diethyl ether in freezer.

Analytical Data of 3-(Cyclopentyloxy)-4-methoxybenzaldehyde O-(2-Morpholin-4-ylacetyl)oxime (6a). Yield: 28%; mp 89–90 °C. ¹H NMR (CDCl₃): δ 1.43–2.13 (m, 8H, 4 CH₂ cyclopent), 2.57–2.78 (m, 4H, 2 CH₂-N morph), 3.39 (s, 2H, CH₂-N), 3.77 (t, J = 4.2 Hz, 4H, 2CH₂-O morph), 3.87 (s, 3H, OCH₃), 4.75–4.92 (m, 1H, CH cyclopent), 6.85 (d, J = 8.2 Hz, 1H, H-5 Ar), 7.24 (dd, J = 1.8, 8.2 Hz, 1H, H-6 Ar), 7.32 (d, J = 1.8 Hz, H-2 Ar), 8.26 (s, 1H, CH=N). IR (KBr): cm^{−1} 1762 (C=O). Anal. Calcd for C₁₉H₂₆N₂O₅.

Synthesis and Analytical Data of Ethyl [(3-(Cyclopentyloxy)-4-methoxyphenyl)methylene]amino]oxy]acetate (11). To a mixture of oxime **8** (1.15 g, 4.9 mmol) and anhydrous potassium carbonate (1.35 g, 9.8 mmol), a solution of ethylbromoacetate (0.65 mL, 5.86 mmol) in dichloromethane (1 mL) was added dropwise at rt. The reaction mixture was heated at 50–60 °C overnight. After cooling, the residue was filtered and washed several times with dichloromethane. The solvent was removed under vacuum, and the crude oil was chromatographed on silica gel (diethyl ether/

petroleum ether 40–60 °C (2:8)) to yield a pure product as pale oil.

Yield 57%. ¹H NMR (CDCl₃): δ 1.27 (t, J = 7.2 Hz, 3H, CH₃), 1.46–2.19 (m, 8H, 4 CH₂ cyclopent), 3.83 (s, 3H, OCH₃), 4.23 (q, J = 7.2 Hz, 2H, CH₃-CH₂), 4.67 (s, 2H, CH₂), 4.70–4.91 (m, 1H, CH cyclopent), 6.80 (d, J = 8.4 Hz, 1H, H-5 Ar), 7.00 (dd, J = 1.8, 8.4 Hz, 1H, H-6 Ar), 7.16 (d, J = 1.8 Hz, H-2 Ar), 8.09 (s, 1H, CH=N). IR (KBr): cm^{−1} 1759 (C=O). Anal. Calcd for C₁₇H₂₃NO₅.

Synthesis and Analytical Data of [(3-(Cyclopentyloxy)-4-methoxyphenyl)methylene]amino]oxy]acetic acid (12). To a solution of **11** (1 g, 3.11 mmol) in ethanol 95% (5 mL), a 2 M NaOH solution (6.22 mL, 12.44 mmol) was added. The reaction mixture was heated at 50–60 °C for 2 h. The solvent was removed under vacuum, and the residue was poured into water and made acid with 1N HCl. The aqueous phase was extracted three times with diethyl ether, dried (MgSO₄), filtered, and evaporated. The obtained oil was chromatographed on silica gel (diethyl ether/petroleum ether 40–60 °C (1:1)) to give a product that was crystallized by diethyl ether/petroleum ether 40–60 °C mixture (1:1).

Yield 75%; mp 91 °C. ¹H NMR (CDCl₃): δ 1.40–2.19 (m, 8H, 4 CH₂ cyclopent), 3.85 (s, 3H, OCH₃), 4.60–4.89 (m, 3H, CH cyclopent + CH₂), 5.70–6.63 (br s, 1H, OH, disappears with D₂O), 6.82 (d, J = 8.2 Hz, 1H, H-5 Ar), 7.00 (dd, J = 1.8, 8.2 Hz,

Table 8. Time of the Collected Fractions and Quantities of the Pure Enantiomer Obtained for **1c**, **2c**, **3c**

compd		impurities ^a	1st enantiomer	intermediate fraction ^b	2nd enantiomer	total (mg)
1c	time (min)	4.40–7.70	7.70–11.19	11.19–12.28	12.28–22.00	
	quantities (mg)	40	164.2	28.2	166.7	399.1
2c	time (min)	3.29–7.00	7.00–12.00	12.00–13.49	13.49–30.00	
	quantities (mg)	80	39.8	70	94.3	284.1
3c	time (min)	3.51–6.29	6.29–6.97	6.97–10.00	10.00–20.00	
	quantities (mg)	23	77.2	56.2	8.8	134

^a Corresponding to the mixture of *Z*(+), *–*)-isomers. ^b Corresponding to the superimposed *E* enantiomers peaks.

Table 9. Enantiomeric Excess and Specific Rotation of the *E* Enantiomers Separated by Semipreparative Chiral HPLC

	compounds	e.e. (%)	α_D^{25a}
1c	1st enantiomer <i>E</i> (+)	98	+13
	2nd enantiomer <i>E</i> (–)	96	–13
2c	1st enantiomer <i>E</i> (+)	> 99	+11
	2nd enantiomer <i>E</i> (–)	> 99	–11
3c	1st enantiomer <i>E</i> (–)	99	–18
	2nd enantiomer <i>E</i> (+)	99	+18

^a Determined in CHCl₃, *c* = 0.1 g/100 mL.

¹H, H-6 Ar), 7.17 (d, *J* = 1.8 Hz, H-2 Ar), 8.11 (s, 1H, CH=N). IR (KBr): cm^{–1} 2500–3500 (OH). Anal. Calcd for C₁₄H₁₇NO₅.

General Procedure for 3-(Cyclopentyloxy)-4-methoxybenzaldehyde *O*-(2-Cycloamin-4-yl-2-oxoethyl) oximes (7a,b**).** To a solution of the intermediate carboxylic acid **12** (2 mmol) in dichloromethane (4 mL), a solution of thionyl chloride (0.17 mL, 2.4 mmol) in dichloromethane (3 mL) was added dropwise at rt and the reaction mixture was refluxed for 4–5 h. The solvent and excess thionyl chloride were removed under reduced pressure. The obtained oil was dissolved in dichloromethane and added to a solution of the suitable amine (morpholine or 2,6-dimethylmorpholine) (2.12 mmol) and anhydrous triethylamine (0.39 mL, 2.8 mmol) in dichloromethane. The reaction mixture was refluxed overnight. After cooling, the mixture was washed twice with brine, dried (MgSO₄), filtered, and evaporated to yield crude oils which were purified by crystallization with diethyl ether (compound **7a**) or by chromatography (Florisil 100–200 mesh, diethyl ether) (compound **7b**).

Analytical Data of 3-(Cyclopentyloxy)-4-methoxybenzaldehyde *O*-(2-Morpholin-4-yl-2-oxoethyl) oxime (7a**).** Yield 75%; mp 99–100 °C. ¹H NMR (CDCl₃): δ 1.43–2.10 (m, 8H, 4CH₂ cyclopent), 3.39–3.72 (m, 8H, 4 CH₂ morph), 3.83 (s, 3H, OCH₃), 4.62–4.90 (m, 3H, CH cyclopent + O-CH₂); 6.80 (d, *J* = 8.3 Hz, 1H, H-5 Ar), 7.00 (dd, *J* = 1.6, 8.3 Hz, 1H, H-6 Ar), 7.16 (d, *J* = 1.6 Hz, H-2 Ar), 8.07 (s, 1H, CH=N). IR (KBr): cm^{–1} 1660 (C=O). Anal. Calcd for C₁₉H₂₆N₂O₅.

Analytical data of compounds **4b–f**, **2a,b**, **3a,b**, **5b**, **6b**, and **7b** are available in Supporting Informations.

Chiral HPLC Analysis of Compounds **1a–c, **2a–c**, **3a–c**.** An analytical study for the separation of the enantiomers was developed for the compounds **1a–c**, **2a–c**, and **3a–c** obtained as racemate in the synthesis.

All the compounds, dissolved in ethanol, were screened on different chiral columns using different mobile phases. The chiral HPLC experiments were performed on a screening unit composed of a Merck D-7000 system manager, Merck-Lachrom L-7100 pump, Merck Lachrom L-7360 oven, which can accommodate 12 chiral columns alimented by a Valco 12 positions valve, Merck-Lachrom 7400 UV detector, and Jasco OR-1590 polarimeter.

The values of the retention time (*R*_t in minutes), the retention factor ($k = (R_t - R_{t0})/R_{t0}$, where *R*_{t0} = 3 was determined by injection of tri-*tert*-butyl benzene) and the enantioselectivity ($\alpha = k_2/k_1$) are reported in Table 6.

All the columns used in the chiral HPLC experiments were polysaccharide based chiral stationary phases (CSPs) except for Whelk-01 (*S,S*). Table 6 collects the experimental procedure used in the screening for each compound.

During the analytical work, we received the biological results for the in vitro pharmacology assays on PDE4 enzyme for the series **1a–b**, **2a–c**, and **3a–c**.

As it is shown in the biological section, interesting results were given by compounds **2c** and **3c** (for compound **1c** the activity was already proved), while all the other compounds of the series **1–3** resulted inactive; so we decided to optimize the analytical conditions of separation only for compounds **1c**, **2c**, and **3c** in order to develop the semipreparative separation.

In Table 7, we report the conditions that allowed a very good separation of the *E*(+) and *E*(–) enantiomers: the chromatograms show good values of retention time, excellent baseline separation, and good resolution. In any case, one observed the presence of one or two minor peaks between 3 and 6 min, which were assigned to the *Z* isomers (HPLC chromatograms are available on Supporting Informations).

Enantiomers Recovery by Semipreparative Separation. All the experiments were performed on a Chiralcel OD (250 mm × 10 mm) column by successive injections on a Knauer unit composed of a Smartline 1000 pump, a Smartline 3900 autosampler, a Smartline 2500 UV detector, and a valve to collect separately the different fractions. The collection procedures used for each compound are reported below.

Compound **1c** (400 mg) was dissolved in hexane/isopropyl alcohol mixture (3:7) (10 mg/mL), and the solution was injected 80 times in portions of 500 μL each (5 mg) every 22 min; the separation was performed by hexane/isopropyl alcohol mixture (3:7), at 30 °C with a flow rate of 5 mL/min; it took about 30 h and needed 9 L of solvent.

Compound **2c** (285 mg) was dissolved in ethanol (19 mg/mL), and the solution was injected 15 times in portions of 1 mL each (19 mg) every 30 min; the separation was performed by ethanol, at 30 °C with a flow rate of 5 mL/min; it took about 7.5 h and needed 2.2 L of solvent.

Compound **3c** (300 mg) was dissolved in ethanol (30 mg/mL), and the solution was injected 20 times in portions of 500 μL each (15 mg) every 40 min; the separation was performed by ethanol, at 30 °C with a flow rate of 5 mL/min; it took about 13 h and needed 4 L of solvent.

In Table 8, we reported the time of the collected fractions and the quantities of the pure enantiomer obtained after solvent evaporation.

The purity control was done on the same HPLC apparatus used in the analytical separation with the same experimental conditions (injected volume: 20 μ L).

The optical rotatory powers of each enantiomer were measured on a 241 MC Perkin-Elmer polarimeter with a sodium lamp (589 nm) and a double-jacketed 10 cm cell at 25 °C.

In Table 9, we showed both the analytical data for the purity control of each enantiomer expressed as enantiomeric excess (e.e.) and the specific rotation (α_D^{25}).

In conclusion, we succeed in obtaining each *E* enantiomers with a good enantiomeric excess and in quantity suitable for the in vitro enzymatic assays, while *Z* enantiomers were not recovered.

Photodensitometric Analysis of Compound 8. To calculate the percentage of *E* and *Z* isomers of compound **8**, we carried out a quantitative photodensitometric analysis after TLC separation by TLSee instruments (GioPharma, srl, Genoa, Italy).

Method. The 3-cyclopentyloxy-4-methoxybenzaldehyde oxime (**8**) (250.0 mg) was solved in absolute ethanol (25.0 mL) obtaining a 10.0 mg/mL solution. Then, 1.0 μ L of analyte solution was spotted on a TLC plate (Silica gel 60 F₂₅₄, Merck, 10 cm \times 10 cm, 1 cm bottom, six spots, each of 10 μ g); the plate was then developed (solvent front = 9 cm) with diethyl ether /petroleum ether 40–60 °C mixture (1:1) as eluent and dried. The plate was finally analyzed by the TLComp apparatus as follows.

After elution, the TLC plate was lighted in a suitable dark-room (TLCam) by a lamp at 254 nm (UV absorption) or 366 nm (fluorescent emission) wavelength and then was photographed by a digital camera. Some TLC image parameters (brightness, contrast, gray scale, multiple releases) can be optimized after and before the acquisition by the TLImage software. In this TLC UV absorption analysis, the spot brightness depends on the energetic radiation of each pixel and corresponds to the sample concentration, the dark being the maximal concentration detectable by the system, while the white corresponds to the analyte's lack. The contrast is a measure of sensibility and the multiple releases (from 1 to 999) make possible an increase of S/N (signal/noise) ratio and LDR (limit of rilevability) optimization. The optimized plate image was then elaborated by a second software, namely TLSee, and converted into a graph like to a typical HPLC chromatogram, where each spot corresponds to a peak and the peak's area gives a quantitative analyte measure.

The plate image after TLImage optimization, the chromatogram obtained by TLSee, a histogram relative to the peak's area of each spots, a table with absolute and percent area values, were reported in Supporting Informations.

Docking Study. The molecular structures of the four **1c** isomers were generated by InsightII (builder module), parametrized according to the CVFF forcefield,²⁹ and their PDE4D complexes were calculated using Autodock 3.05.³⁰

The model of the PDE4D enzyme was derived by the crystal structure of the PDE4D/Cilomilast complex (PDB code 1XOM) according to the following protocol: (i) the crystal structures of the available PDE4B and D/ligand complexes (PDB codes: 1XOM, 1XLZ, 1XON, 1Y2D, 1XOT, 1Q9M, 1OYN) were superimposed (lsqkab program, CCP4 suite) using the C α atoms; (ii) the PDE4 binding site was visually inspected and the water molecules conserved in all the analyzed structures (as well as the metal ions) were

inserted in the protein model and used for docking calculation; (iii) the 1XOM coordinates were selected (being the highest resolution model) and Cilomilast was removed from the binding site; (iv) hydrogen atoms were added and partial charges were assigned according to CVFF forcefield (Insight II, biopolymer module).

The ligand "root" was defined automatically and all bonds were allowed to freely rotate. A 60 \times 60 \times 60 grid (grid spacing 0.375 Å) was centered on the ligand binding site and electrostatic and affinity maps for each atom type of the ligand were calculated. The docking search was performed using the genetic algorithm local search protocol as implemented in AutoDock (number of runs: 10; number of individuals in population: 150; rate of gene mutation: 0.02; rate of crossover: 0.8). The docking poses were clustered (rmsd 2.0 Å), and the best conformation of the low energy, highest populated cluster was selected as the binding conformation.

All the calculations were carried out on Silicon Graphic Indigo2 and Origin 200 workstations. Model analyses were performed using the CCP4 program suite.³¹ The programs Molscript³² and Raster3D³³ were used to draw the figures.

Enzyme Assays. PDE4 and PDE4D. PDE4 and PDE4D enzyme assays were performed by CEREP (Celle L'Evescault, France), using standard procedures as reported in the literature. Particularly, PDE4 assays were performed using enzyme purified from human monocyte (U-937);²⁶ PDE4D tests were carried out on human recombinant PDE4D obtained from Sf9 cells.²⁷ In all the experiments, rolipram as reference compound was tested at nine concentrations, in duplicate, to obtain an inhibition curve in order to validate this experiment. Title compounds were solved in DMSO at 10⁻² M concentration and then diluted with water to the final suitable concentrations. All the compounds were tested preliminary at 10⁻⁵ M concentration, in duplicate. Results are expressed as a percent inhibition of control activity. Results showing an inhibition of the control higher than 50% are considered to represent significant effects of the test compounds. 50% is the most common cutoff value for further investigation (determination of IC₅₀ value from concentration–response curves).

Compounds showing inhibition control higher than 50% were further tested at five concentrations in the interval 5 \times 10⁻⁸–10⁻⁴ M. IC₅₀ values for rolipram and tested compounds were determined by nonlinear regression analysis of its inhibition curve, using Hill equation curve fitting (Graph Pad Prism software). The IC₅₀ values obtained for the reference compounds are within accepted limits of historic averages obtained \pm 0.5 log unit. The IC₅₀ values and the relative Fiducial intervals at 95% confidence for each tested compounds were reported at μ M concentration (Tables 1 and 2).

PDE4 Subtype Assays by IMAP Methods. PDE4A4, PDE4B2, PDE4C2, and PDE4D1–D3 enzyme assays were performed by Scottish Biomedical (Glasgow, Scotland, UK) using recombinant human PDE enzymes expressed in a baculoviral system. The preliminary screening assays were performed by the IMAP technology (Molecular Devices), which is based on the high affinity binding of phosphate by immobilized metal coordination complexes on nanoparticles. The binding reagent complexes with phosphate groups on nucleotide monophosphate generated from cyclic nucleotides (cAMP) through phosphodiesterases. With fluorescence polarization detection, binding causes a change in

the rate of the molecular motion of the phosphate bearing molecule and results in an increase in the fluorescence polarization value observed for the fluorescent label attached to the substrate.

As for PDE4 and PDE4D tests, compounds **4a**, **5b**, **6b**, and **7b** were preliminary tested at 10 μ M concentration in duplicate (Table 3), then compounds **4a**, **5b**, and **7b** were tested by the same IMAP method on PDE4D3, at further five concentrations from 10^{-4} to 10^{-8} M, and IC₅₀ values were determined by nonlinear regression analysis of its inhibition curve (GraphPad Prism software) (Table 4).

PDE4D1, PDE4D2, PDE4D3 Assays by Radiometric Method. An additional study on compound **4a** was performed to verify its antagonist activity on PDE4D1, PDE4D2, and PDE4D3 and to determine its IC₅₀ and K_i values.

The phosphodiesterase assays were performed using recombinant human PDE4D1, PDE4D2, and PDE4D3 enzymes expressed in a baculoviral system (0.5 U/ μ L in 20 mM Tris-HCl pH 7.4) (1 unit converts 1 pmol of cAMP to AMP per min at 30 °C, pH 7.4). The enzyme concentration used for the inhibition assay is one that has been previously identified as producing activity at the high end of the linear range. These enzymes were tested for their similarity to PDE enzymes taken from human tissue using known inhibitor standard (rolipram). The radiometric assay is a modification of the two-step method of Thompson and Appleman,²⁸ adapted for 96-well plate format. **4a** and rolipram, as reference compound, were dissolved in 100% DMSO at a concentration of 10 mM. All subsequent assays were performed in 5% DMSO (final). The compounds were tested by performing a serial dilution at a starting concentration of 100 μ M to a final concentration of 1 nM, in duplicate. Enzyme solution was incubated in each plate well with cAMP solution (1 μ M) as substrate, [³H]-cAMP as tracer, and the test compounds for 20 min at 30 °C. The enzyme was denatured by incubation for 2 min at 70 °C, and the [³H]-5'-AMP was converted in [³H]-adenosine by addition of snake venom nucleotidase. Uncleaved cyclic nucleotide substrate was removed by Dowex resin solution. After centrifugation, the supernatant was added to a scintillant plate containing 200 μ L of Microscint-20 for well. The level of reaction product (labeled phosphate) was finally detected with a scintillation counter and plotted as CPM values against the logarithm of inhibitor's concentration to generate the dose-response curves (Prism software, GraphPad Inc.) from which the IC₅₀ values were calculated.

A control solution containing 11 μ L of DMSO, 50 μ L of ³H-cAMP, and 50 μ L of enzyme per well, and blank solutions being the same as the control without enzyme, were used in each assay. Basing on the close structural relation with our lead compound **1c**, we assume that compound **4a** is a competitive inhibitor of PDE4D1, PDE4D2, and PDE4D3, and we calculated the K_i values from the IC₅₀ values using the Cheng-Prusoff equation: IC₅₀ = K_i (1 + [S]/K_m) (Table 5).

Acknowledgment. We thank Dr. R. Raggio, O. Gagliardo, and F. Tuberoni for spectral recording and Prof. M. Bradley for English revision of the text. We give a particular acknowledgement to Prof. G. Amandola, who provided us the TLSee Instrument for photodensitometric analysis. Financial support from MIUR (Minister of University and Research, PRIN grant 2005032713-005) is gratefully acknowledged.

Supporting Information Available: Analytical data of compounds **4b–f**, **2a,b**, **3a,b**, **5b**, **6b**, and **7b**. ¹H NMR spectra of each isomer of compound **8**. HPLC chromatograms of compounds **1c**, **2c**, and **3c** as racemate and as pure enantiomers. Figures and table relative to the photodensitometric analysis of compound **8**. This material is available free of charge via the Internet at <http://pubs.acs.org>.

References

- (1) Siegelbaum, S. A.; Schwartz, J. H. Modulation of synaptic transmission: second messengers. In *Principles of Neural Science*; Kandel, E. R., Schwartz, J. H., Jessel, T. M., Ed.; McGraw-Hill Press: New York, 2000; pp 229–252.
- (2) Dudai, Y. Cyclic AMP and learning in *Drosophila*. *Adv. Cycl. Nucleic Protein Phosphoryl. Res.* **1986**, *20*, 343–361.
- (3) Morimoto, B. H.; Koshland, D. E., Jr. Identification of cyclic AMP as the response regulator for neurosecretory potentiation: a memory model system. *Proc. Natl. Acad. Sci. U.S.A.* **1991**, *88*, 10835–10839.
- (4) Bonkale, W. L.; Cowburn, R. F.; Ohm, T. G.; Bogdanovic, N.; Fastbom, J. A quantitative autoradiographic study of [³H]cAMP binding to cytosolic and particulate protein kinase A in post-mortem brain staged for Alzheimer's disease neurofibrillary changes and amyloid deposits. *Brain Res.* **1999**, *818*, 383–396.
- (5) Cowborn, R. F.; Fowler, C. J.; O'Neill, C. Neurotransmitters, signal transduction and second-messengers in Alzheimer's disease. *Acta Neurol. Scand. Suppl.* **1996**, *165*, 25–32.
- (6) Zhang, H. T.; Crispass, A. M.; Dorairaj, N. R.; Chandler, L. J.; O'Donnel, J. M. Inhibition of cyclic AMP phosphodiesterase (PDE4) reverses memory deficits associated with NMDA receptor antagonism. *Neuropsychopharmacology* **2000**, *23*, 198–204.
- (7) Survana, N. U.; O'Donnel, J. M. Hydrolysis of *N*-methyl-D-aspartate receptor-stimulated cAMP and cGMP by PDE4 and PDE2 phosphodiesterases in primary neuronal cultures of rat cerebral cortex and hippocampus. *J. Pharmacol. Exp. Ther.* **2002**, *302*, 249–256.
- (8) Blokland, A.; Schreiber, R.; Prickaerts, J. Improving memory: a role for phosphodiesterases. *Curr. Pharm. Des.* **2006**, *12*, 2511–2523.
- (9) Zhang, H. T.; Zhao, Y.; Huang, Y.; Dorairaj, N. R.; Chandler, L. J.; O'Donnel, J. M. Inhibition of phosphodiesterase 4 (PDE4) enzyme reverses memory deficits produced by infusion of MEK inhibitor U0126 into the CA1 subregion of the rat hippocampus. *Neuropsychopharmacology* **2004**, *29*, 1432–1439.
- (10) Zhang, H. T.; O'Donnel, J. M. Effect of rolipram on scopolamine-induced impairment of working and reference memory in the radial-arm maze test in rats. *Psychopharmacology (Berlin)* **2000**, *150*, 311–316.
- (11) Rutten, K.; Prickaerts, J.; Blokland, A. Rolipram reverse scopolamine-induced and time-dependent memory deficits in object recognition by different mechanism of action. *Neurobiol. Learn. Mem.* **2006**, *85*, 132–138.
- (12) Schoffeleers, A. N.; Wardeh, G.; Mulder, A. H. Cyclic AMP facilitates the electrically evoked release of radiolabelled noradrenaline, dopamine and 5-hydroxytryptamine from rat brain slices. *Naunyn-Schmiedeberg's Arch. Pharmacol.* **1985**, *330*, 74–76.
- (13) Masliah, E. Mechanisms of synaptic dysfunction in Alzheimer's disease. *Histol. Histopathol.* **1995**, *10*, 509–519.
- (14) Gong, B.; Vitolo, O. V.; Trinchese, F.; Liu, S.; Shelanski, M.; Arancio, O. Persistent improvement in synaptic and cognitive functions in an Alzheimer mouse model after rolipram treatment. *J. Clin. Invest.* **2004**, *114*, 1624–1634.
- (15) Rutten, K.; Prickaerts, J.; Schaenle, G.; Rosenbrock, H.; Blokland, A. Subchronic rolipram treatment leads to a persistent improvement in long-term object memory in rats. *Neurobiol. Learn. Mem.* **2008**, *90*, 569–575.
- (16) Houslay, M. D. PDE4 cAMP-specific phosphodiesterases. *Prog. Nucleic Acid Res. Mol. Biol.* **2001**, *69*, 249–315.
- (17) Chandrasekaran, A.; Toh, K. Y.; Low, S. H.; Hong Tay, S. K.; Brenner, S.; Li Meng Goh, D. Identification and Characterization of novel mouse PDE4D isoforms: Molecular cloning, subcellular distribution and detection of isoform-specific intracellular localization signals. *Cell. Signalling* **2008**, *20*, 22139–22153.
- (18) Lynex, C. N.; Chen, M. L.; Toh, K. Y.; Low, R. W. C.; Goh, D. L. M.; Hong Tay, S. K. Identification and molecular characterization of a novel PDE4D11 cAMP-specific phosphodiesterase isoform. *Cell. Signal.* **2008**, *20*, 2247–2255.
- (19) Houslay, M. D.; Adams, D. R. PDE4 cAMP phosphodiesterases: modular enzymes that orchestrate signalling cross-talk, desensitization and compartmentalization. *Biochem. J.* **2003**, *370*, 1–18.

- (20) MacKenzie, S. J.; Baillie, G. S.; McPhee, I.; MacKenzie, C.; Seamons, R.; McSorley, T.; Millen, J.; Beard, M. B.; van Heeke, G.; Housley, M. D. Long PDE4 cAMP specific phosphodiesterases are activated by protein kinase A-mediated phosphorylation of a single serine residue in upstream conserved region 1 (UCR1). *Br. J. Pharmacol.* **2002**, *136*, 421–433.
- (21) Hill, E. V.; Sheppard, C. L.; Cheung, Y. F.; Gall, I.; Krause, E.; Houslay, M. D. Oxidative stress employs phosphatidyl inositol 3-kinase and ERK signalling pathways to activate cAMP phosphodiesterase-4D3 (PDE4D3) through multisite phosphorylation at Ser239 and Ser579. *Cell. Signalling* **2006**, *18*, 2056–2069.
- (22) Zhang, H. T.; Huang, Y.; Survana, N. U.; Deng, C.; Crissman, A. M.; Hopper, A. T.; De Vivo, M.; Rose, G. M.; O'Donnel, J. M. Effects of the novel PDE4 inhibitors MEM1018 and MEM1091 on memory in the radial-arm maze and inhibitory avoidance tests in rats. *Psychopharmacology* **2005**, *179*, 613–619.
- (23) Bruno, O.; Brullo, C.; Arduino, N.; Schenone, S.; Ranise, A.; Bondavalli, F.; Ottonello, L.; Dapino, P.; Dallegri, F. Synthesis and biological evaluation of neutrophilic inflammation inhibitors. *Farmaco* **2004**, *59*, 223–235.
- (24) Ashton, M. J.; Cook, D. C.; Fenton, G.; Karlsson, J. A.; Palfreyman, M. N.; Raeburn, D.; Ratcliffe, A. J.; Souness, J. E.; Thurairatnam, S.; Vicker, N. Selective type IV phosphodiesterase inhibitors as antiasthmatic agents. The syntheses and biological activities of 3-(cyclopentyloxy)-4-methoxybenzamides and analogues. *J. Med. Chem.* **1994**, *37*, 1696–1703.
- (25) McCarty, C. G. *Syn-anti* isomerization and rearrangements. In: *The Chemistry of the Carbon–Nitrogen Double Bond*. Patai, S., Ed.; Wiley and Sons: New York, 1970; pp 363–464.
- (26) Torphy, T. J.; Zhou, H. L.; Cieslinski, L. B. Stimulation of beta adrenoreceptors in a human monocyte cell line (U937) up-regulates cyclic AMP-specific phosphodiesterase activity. *J. Pharmacol. Exp. Ther.* **1992**, *263*, 1195–1205.
- (27) Saldou, N.; Obernolte, R.; Huber, A.; Badcker, P. A.; Wilhelm, R.; Alvarez, R.; Li, B.; Xia, L.; Callan, O.; Su, C.; Jargin, K.; Shelton, E. R. Comparison of recombinant human PDE4 isoforms: interaction with substrate and inhibitors. *Cell. Signalling* **1998**, *10*, 427–440.
- (28) Thompson, W. J.; Appleman, M. M. Multiple cyclic nucleotide phosphodiesterase activities from rat brain. *Biochemistry* **1971**, *10*, 311–316.
- (29) Dauber-Osguthorpe, P.; Roberts, V. A.; Osguthorpe, D. J.; Wolff, J.; Genest, M.; Hagler, A. T. Structure and energetics of ligand binding to proteins: *Escherichia coli* dihydrofolate reductase-trimethoprim, a drug-receptor system. *Proteins* **1988**, *4*, 31–47.
- (30) Morris, G. M.; Goodsell, D. S.; Halliday, R. S.; Huey, R.; Hart, W. E.; Belew, R. K.; Olson, A. J. Automated docking using a Lamarckian genetic algorithm and an empirical binding free energy function. *J. Comput. Chem.* **1998**, *19*, 1639–1662.
- (31) The CCP4 suite: programs for protein crystallography. Collaborative Computational Project, Number 4. *Acta Crystallogr., Sect. D: Biol. Crystallogr.* **1994**, *50*, 760–763.
- (32) Kraulis, P. J. MOLSCRIPT: a program to produce both detailed and schematic plots of protein structures. *J. Appl. Crystallogr.* **1991**, *24*, 946–950.
- (33) Esnouf, R. M. An extensively modified version of MolScript that includes greatly enhanced coloring capabilities. *J. Mol. Graphics Modell.* **1997**, *15*, 132–134.